THE JOURNAL OF PHYSICAL CHEMISTRY B

Article

pubs.acs.org/JPCB

Slow Relaxation Dynamics of Water in Hydroxypropyl Cellulose-Water Mixture Traces Its Phase Transition Pathway: A Spectroscopic Investigation

Animesh Patra,[†] Pramod Kumar Verma,[†] and Rajib Kumar Mitra*[,†]

[†]Unit for Nano Science & Technology, Department of Chemical Biological and Macromolecular Sciences, S.N. Bose National Centre for Basic Sciences, Block JD, Sector III, Salt Lake, Kolkata 700098, India

ABSTRACT: In this study, we have explored the slow (of the order of several hundreds of picoseconds) relaxation dynamics of water associated with the hydration shell of a biocompatible polymer, hydroxypropyl cellulose (HPC)-water mixture as a function of HPC concentration using time-resolved fluorescence spectroscopy. The relaxation dynamics slows down with a progressive increase in HPC content indicating restriction of the relaxation pathway of water molecules specially beyond a cellulose concentration of 20% wherein an isotropic to liquid crystalline cholesteric microscopic phase separation sets in. The activation energy calculated from the temperature dependent solvation dynamics studies also shows a similar trend. The nucleophilic activity of water molecules in these mixtures is determined by measuring the reaction kinetics of solvolysis of benzoyl chloride, and the reaction rate exhibits a marked decrease as the phase separation sets in. The observed results are correlated with a transition between the 'bulk' and 'bound' type of water molecules present in the system.

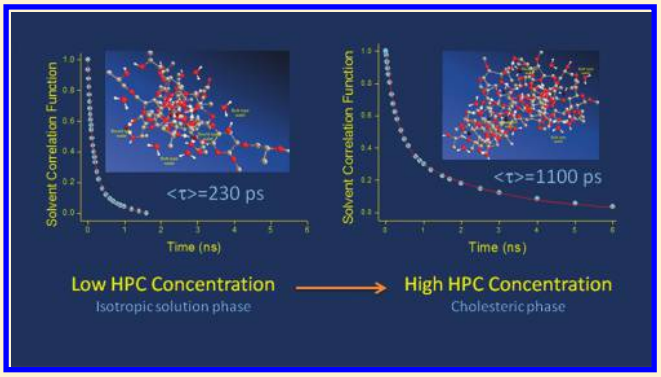

INTRODUCTION

Water in a restricted environment has always been a fascinating area of research as it furnishes properties of water markedly different from those of bulk water, specially in biologically relevant environments.[1,2] In this regard biopolymer−water mixtures[3−11] are of potential interest since these systems provide a potential environment that mimics real biological systems. Hydroxypropyl cellulose[12] (HPC) is a well studied biopolymer which shows excellent biodegradability and biocompatibility, electroneutrality, and high water solubility.[8,11,13−25] It is a recommended food additive and finds usage in foods as an emulsifier and encapsulator. In this respect the study of hydration structure and dynamics in the HPC-water mixture is strongly demanding in view of its fruitful applications. A HPC molecule is known to adopt a helical conformation in the crystalline state;[26,27] however, its conformation in aqueous solution and liquid crystalline phase is rather complex. At low HPC concentration an isotropic phase dominates,[13] and it forms an ordered liquid crystalline phase with cholesteric structure at about 40 wt % polymer in water. The structural transition is not a sharp one, and an onset of the phase transition sets off at a relatively lower concentration. The polymer is soluble in cold water, and when the aqueous solution is warmed to ∼40 °C, a phase separation occurs with a sharp increase in turbidity and a decrease in viscosity. Phillips et al.[19] reported a detailed measurement of the low shear viscosity of HPC in aqueous solution and identified a transition in viscosity dependency on HPC concentration, and the transition relates a structural modification of HPC with concentration. Fluorescence recovery after photobleaching (FRAP) studies[18,24] using different dye molecules have identified a decrease in diffusion coefficient and an increase in microviscosity with an increase in HPC concentration. Immanei et al.[22] reported on the effect of structure and temperature on the rheo-optic behavior of HPC solution in water by measuring flow birefringes and intrinsic viscosity, and the observed effects are related to the structural features in the chain backbone. Yakimet et al.[11] reported the effect of water content on the structural recognition and elastic properties of HPC films using FTIR, differential scanning calorimetry (DSC), and X-ray diffraction techniques. They reported the elasticity of the film to be strongly dependent on the water content, and even a small increase in the water content led to a relatively large decrease in the elasticity modulus. Wojciechowski et al.[25] studied the nature of water molecules in HPC hydrogel with liquid crystalline (LC) organization using DSC and dielectric relaxation (DR) techniques. They identified two distinct types of water species to be present in the hydrogel. The first type is a 'bound type' water molecule which is constrained in the LC polymer network. The second type is 'bulk type' water adsorbed in the pores of LC environment.

Received: September 22, 2011
Published: January 19, 2012

The dynamics of water in the HPC-water mixture has previously been studied with a dielectric relaxation (DR) technique.[8,9,21,25,28] These studies conclude that the mobility and hence the alignment of molecular chains in the disordered regions of HPC, responsible for dielectric polarization, depend not only on the amount of water present but also on the mode of interaction between water molecules and cellulose chain. Also during thermal treatment the removal of water molecules from the disordered regions results in some changes in the intermolecular interaction between adjacent cellulose chains. The adsorbed water molecules in cellulose could be differentiated into 'free type' or loosely bound type and tightly 'bound' type, and that different modes of interactions may occur depending on the amount of water in a given solution.[17] At low water content the bound water molecules may associate with the polar OH groups of cellulose chains or form cross-link between chains. When the number of sites available for these tightly bound water molecules is consumed, additional water molecules are bound loosely in such a manner so as these water molecules do not further enhance the dielectric loss mechanism. The activation energy of the relaxation process due to the bound type water, as observed in the MHz region, is observed to decrease with decreasing the moisture content.[8] Recently Sudo et al.[21] have studied the primary relaxation process due to the motion of "free water" restricted by HPC molecules as observed in the GHz region at different HPC concentrations and temperatures. The relaxation process is observed to slow down with increasing HPC concentration with a clear transition at 23 wt % HPC content wherein, according to the authors, lies the onset of the isotropic to a collesteric structural phase transition of the mixture. Such a phase transition involves the release of a fraction of hydrogen bonded water molecules in the form of "free water". The activation energy has also been observed to increase beyond 23 wt % HPC to reach a value similar to that of the hydrogen bonded energy in bulk water. It is important to note here that at the onset of the cholesteric phase, a fraction of water molecules still remains restricted in the structured HPC network, and it is rather interesting to understand how this restriction modifies the dynamics of water. Our present investigation is thus motivated to underline the slow dynamics of these water molecules in the HPC-water mixture, and its manifestation as the biopolymer solution changes its phase.

We have used the picoseconds-resolved fluorescence spectroscopic technique to underline the dynamics of water at six different HPC concentrations of 10, 15, 20, 25, 30, and 40 wt % in water at four different temperatures of 273, 283, 293, and 303 K. This study complements our previous investigations on the mode of slow solvation dynamics produced by confined water in microheterogeneous assemblies and the corresponding energetics of the cross over between 'bound' and 'free' type of water molecules present in such systems.[29−34] The choice of the composition and temperature range is based on the isotropic solution limit as obtained from previously reported phase diagrams.[16] The focus of our study to identify the possible modification of slow solvent relaxation dynamics associated with a change in the microscopic phase morphology at ∼20% HPC also influences the choice of the compositions. Coumarin-500 (C-500) is used as the fluoroprobe, which has the potential to provide information selectively from microheterogeneous interfaces.[30] Steady state emission and excitation measurements provide information on the micropolarity of the immediate environment of the fluorophore. The geometrical restriction on the probe is determined with the help of ps-resolved rotational anisotropy study. Finally the activity of water in these solutions is determined by measuring the kinetics of the solvolysis reaction of benzoyl chloride. Our studies clearly demonstrate that water dynamics traces the phase transition pathway of the HPC-water mixture, and activity of the restricted water molecules in the solution gets modulated accordingly.

MATERIALS AND METHODS

Hydroxyl propyl cellulose (HPC), weight-average molecular mass, M_W = 80000 [Scheme 1] was purchased from Aldrich.

Scheme 1. Molecular Structure of the Probe Coumarin 500 (C-500) and Hydroxypropyl Cellulose (HPC)

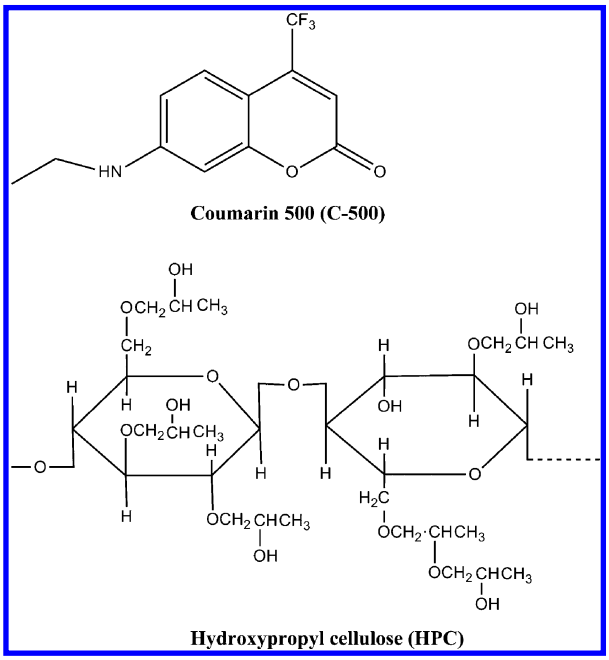

Benzoyl chloride (BzCl) was purchased from Merck. Coumarin-500 (C-500) [Scheme 1] was a product of Exciton. All these chemicals were used without further purification. A very dilute solution of C-500 in water (∼1 μM) was made, and 20 μL of that solution was added into HPC prior to the addition of calculated volume of (Millipore) water, followed by vigorous stirring for 8 days and 3 days of equilibration at 293 K. Steady-state emission and excitation spectra were measured in a Jobin Yvon Fluorolog-3 fluorimeter with a Peltier controlled temperature attachment. Time-resolved fluorescence measurements were performed on a commercially available spectrophotometer (LifeSpec-ps) from Edinburgh Instrument, U.K. (excitation wavelength 409 nm, 80 ps instrument response function (IRF)) with a temperature controlled attachment from Julabo (Model: F32). Fluorescence transients were fitted by using software F900 from Edinburgh Instruments. The phenomenon 'solvation' refers to the stabilization of a solute molecule because of its interaction with the surrounding solvent molecules. The dynamics of this process, i.e., how quickly the solvent dipoles rearrange around an instantaneously created charge (electron) or dipole, is known as solvation dynamics. When a fluorophore in a solution is excited by an ultrashort light pulse (ps or fs duration) at time t = 0, a dipole is created instantaneously. This dipole gives rise to an

dx.doi.org/10.1021/jp300428h | J. Phys. Chem. B 2012, 116, 1508−1516

instantaneous electric field on the solvent molecules. Due to the interaction of the solvent dipoles with the electric field, the free energy minimum of the solvent shifts to a nonzero value of the polarization. Since the fluorophore is excited instantaneously, the solvent molecules at $t = 0$ find themselves in a relatively high energy configuration. Subsequently, the solvent molecules begin to move and rearrange themselves to reach their new equilibrium positions. As time increases, the solvent dipoles gradually reorient, and the energy of the excited dipole decreases. Thus, with an increase in time the emission maximum shifts to lower energy, i.e., toward longer wavelength. This phenomenon is known as time dependent fluorescence Stokes shift (TDFSS). The details of the time-resolved measurements could be found elsewhere.[29] The time-dependent fluorescence Stokes shifts, as estimated from TRES (time-resolved emission spectra), were used to construct the normalized spectral shift correlation function or the solvent correlation function, $C(t)$, defined as

$$C(t) = \frac{\nu(t) - \nu(0)}{\nu(\infty) - \nu(0)} \quad (1)$$

where $\nu(0)$, $\nu(t)$, and $\nu(\infty)$ are the emission maxima (in cm^{-1}) at time zero, t, and infinity, respectively. The $\nu(\infty)$ values have been taken to be the emission frequency beyond which an insignificant or no spectral shift is observed. The $C(t)$ function represents the temporal response of the solvent relaxation process, as occurs around the probe following its photoexcitation and the associated change in the dipole moment. For rotational anisotropy ($r(t)$) measurements, emission polarization was adjusted to be parallel or perpendicular to that of the excitation, and anisotropy is defined as

$$r(t) = \frac{[I_{para} - GI_{perp}]}{[I_{para} + 2GI_{perp}]} \quad (2)$$

where G is the grating factor determined following a long-time tail matching technique.[35] The kinetics of BzCl solvolysis reaction was determined by measuring the temporal change in the absorbance of BzCl monitored at 288 nm using a Shimadzu UV-2450 spectrophotometer. The rate of the reaction was calculated using a first order exponential fit of the absorbance data. The initial BzCl concentration was kept constant at ~10 μM.

RESULTS AND DISCUSSION

Figure 1(a, b) depicts the emission and excitation spectra of C-500 in the HPC-water mixture at different representative HPC concentrations (10, 20, 30, and 40%) measured at 293 K. As evidenced from Figure 1a, the emission spectrum shows a progressive blue shift with increasing HPC concentration. C-500 in water produces an emission peak (λ_{em}^{max}) at 506 nm, and for 40% HPC, the emission peak is blue-shifted to 495 nm. We plot the relative shift of λ_{em}^{max} (with respect to that of water) against HPC concentration (Figure 1a, inset), and it is found that the relative shift in λ_{em}^{max} changes rapidly at and beyond 20% HPC concentration. The decreased polarity of the system as experienced by the probe molecule with increasing HPC concentration is reflected in the blue shift of λ_{em}^{max}, a phenomenon comparable to that found in AOT reverse micellar (RM) systems with decreasing water content.[30] In order to get a deeper insight we measure the excitation spectra of the same systems (Figure 1b). It is found that in water C-500

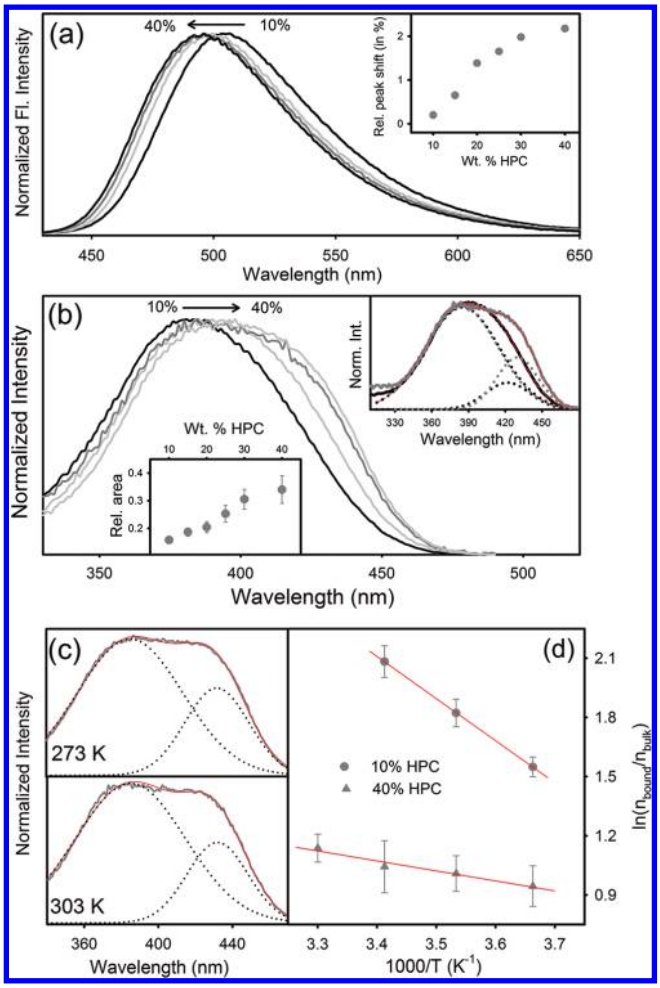

Figure 1. (a) Emission spectra of C-500 at 293 K in the HPC-water mixture with HPC weight percentage of 10, 20, 30, and 40%. A progressive blue shift of the emission peak is observed with increasing HPC concentration. The relative peak shift with respect to that in water against HPC concentration is shown in the inset. (b) Excitation spectra of C-500 at 293 K in the HPC-water mixture with HPC weight percentage of 10, 20, 30, and 40%. The upper inset shows deconvoluted spectra of 10% (black) and 40% (gray) HPC-water mixtures. The red solid lines are the overall fittings. The relative area of the second curve with respect to that of the first one is plotted against HPC concentration in the lower inset. (c) Deconvoluted excitation spectra C-500 in 40% HPC solution at 273 and 303 K. The red solid line is the overall fit, while the dotted lines are the deconvoluted fits. (d) Plot of $\ln(n_{bound}/n_{bulk})$ against $1/T$ for 10% and 40% HPC solutions. The red solid lines are the linear fits.

produces an excitation peak at 390 nm (data not shown), which is consistent with earlier reports for the identical system.[36] With increasing HPC concentration the excitation peak suffers a progressive red shift coupled with an increasing FWHM of the observed spectrum. This broadening could be envisaged as a possible distribution of the probe molecules in different microenvironments in the mixture with a notion that a fraction of the probe is exposed to the bulk type water whereas the rest probes a restricted environment, which has been reported to absorb at a higher wavelength.[30,37] We therefore deconvolute the observed excitation spectra into two separate spectra with one peak fixed at 390 nm. Representative deconvoluted figures for 10% and 40% HPC-water solution are presented in the upper inset (Figure 1b). As evidenced from the figure, for 10%

dx.doi.org/10.1021/jp300428h | J. Phys. Chem. B 2012, 116, 1508−1516

HPC the second peak appears at 422 nm and for 15, 20, 25, 30, and 40% HPC, the peak suffers progressive red shift to appear at 425, 427, 427, 428, and 429 nm, respectively. It could be intuited that while the first peak arises due to the distribution of C-500 in the bulk aqueous environment (centered at 390 nm), the second one is due preferably to the C-500 residing in the hydrophobic environment of HPC. The area under each curve could well correspond to the number of water molecules belonging to that particular 'species'. We, therefore, plot the relative ratio of the area under the two curves against HPC concentration (Figure 1b, lower inset). A progressive increase in the area of the second curve comprehends the increased fraction of C-500 residing in the interfacial region of HPC-water system at lower hydration. The observed red shift in the excitation spectra can be explained in terms of the relative increase in the hydrophobicity of the system with increasing content of HPC which reduces the dipole−dipole interaction of the solvent-fluorophore, thereby stabilizing it. The curve shows a change in slope beyond 20% HPC which in turn corresponds to the onset of phase transition of the polymer as it turns hydrophobic at and beyond this concentration.[21]

We now switch to the time-resolved study. Figure 2 (upper inset) shows representative fluorescence transients of the probe

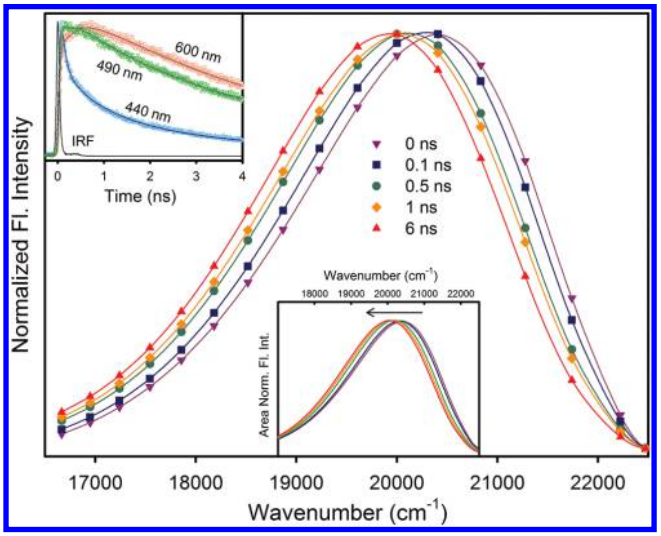

Figure 2. (Upper inset) A representative decay transient of C-500 in 30% HPC-water mixture at 293 K measured at three wavelengths, viz. 440, 490, and 600 nm. The solid lines are the multiexponential fits of the curves. (Main figure) Time resolved emission spectra (TRES) of C-500 in 30% HPC-water mixture at 293 K. A representative time-resolved area normalized emission spectra (TRANES) for 30% HPC solution at 293 K is presented in the lower inset. The arrow indicates increase in time.

C-500 in 30% HPC-water mixture at three selected wavelengths of 440, 490, and 500 nm studied at 293 K. The 440 nm decay transient can triexponentially be fitted with the time constants of 0.11 ns (57%), 1.02 ns (25%), and 4.44 ns (18%), whereas, for the 600 nm transient, a distinct rise component of 0.45 ns is obtained along with a decay component of 4.9 ns. Similar wavelength dependent transient fittings are also been obtained in solutions with other mixtures. Such wavelength dependency clearly indicates solvation of the fluoroprobe. In order to estimate the solvation relaxation rate, we construct time-resolved emission spectra (TRES) for different HPC-water mixtures using the fitting parameters of the transients and following the procedure described elsewhere.[29] A representative TRES of 30% HPC-water mixture at 293 K has been shown in Figure 2. It is observed that the spectrum suffers progressive red shift with time. We first need to ensure that the observed time-resolved shift in the emission spectra is not concerned with any internal photophysics associated with the probe itself, and it remains as a single species throughout. We therefore construct the time-resolved area normalized emission spectra (TRANES)[38] for all the samples and a representative TRANES for 30% HPC at 293 K is depicted in Figure 2 (lower inset). Existence of an iso-emissive point in a TRANES profile specifies that the observed emission from the probe is due to two different 'species' of the probe, irrespective of their origin. As evidenced from the figure, no iso-emissive point is apparent for any of these systems and this therefore affirms that the observed dynamics is due solely to a single probe species, and any modulation is caused only due to the heterogeneity in the location of the probe.

Solvent correlation function, $C(t)$ are constructed for all the systems following eq 1. All these curves are fitted biexponentially (Figure 3a) using the equation $C(t) = a_1 \exp(-t/\tau_1) + a_2 \exp(-t/\tau_2)$ where τ_1 and τ_2 are the two associated time scales and a_i's are their corresponding weightages. All the corresponding fitting parameters are presented in Table 1. It is evident from the table that one of the solvation time constants is of the order of a few hundreds of picoseconds (ps), while the other one extends from hundreds of ps to a few nanoseconds (ns). The two time scales essentially correspond to the different modes of coupled translational and rotational motion of the two different types of water molecules present at the HPC-water interface. The observed time scales are comparable with those obtained in the case of the polyethylene glycol-water mixture,[32] AOT RM systems,[30] and AOT lamellar systems[34] using the same probe molecule. It is worth mentioning here that C-500 in water produces ultrafast solvation time scales of 300 and 700 fs.[36] Our instrumental resolution (80 ps IRF) limits us to miss a considerable part of the fluorescence signal. To make an estimate of the loss in the fluorescence signal we determine the time zero frequency of the fluorescence spectrum maximum, $\nu^{p}_{em}(0)$ from the following equation[39]

$$\nu^{p}_{em}(0) = \nu^{p}_{abs} - [\nu^{np}_{abs} - \nu^{np}_{em}] \quad (3)$$

where ν^{p}_{abs}, ν^{np}_{abs}, and ν^{np}_{em} are the absorption peak of the fluorophore in polar solvent, absorption peak in nonpolar solvent, and emission peak in nonpolar solvent, respectively. Considering cyclohexane to be the nonpolar solvent in which C-500 produces absorption and emission peaks at 360 and 410 nm, respectively, and water to be the polar solvent, we estimate at the best ~30% recovery of the total fluorescence signal. Our instrumental resolution is far beyond to probe the fast time-scale associated with the ultrafast water relaxation process; however, the essence of this study is focused on the slow dynamics of water, and, therefore, the observed loss of the ultrafast fluorescence signal does not significantly affect the conclusion drawn.

As observed from Table 1, the average solvation time constant $\langle\tau\rangle$ ($= a_1\tau_1 + a_2\tau_2$) increases gradually with increasing HPC concentration in the mixture. A similar retardation of the relaxation process of the dielectric with an increase of the polymer fraction has previously been reported in HPC-water[21] and ethyleneglycol-dioxane[40] mixtures. Our study, however,

dx.doi.org/10.1021/jp300428h | J. Phys. Chem. B 2012, 116, 1508−1516

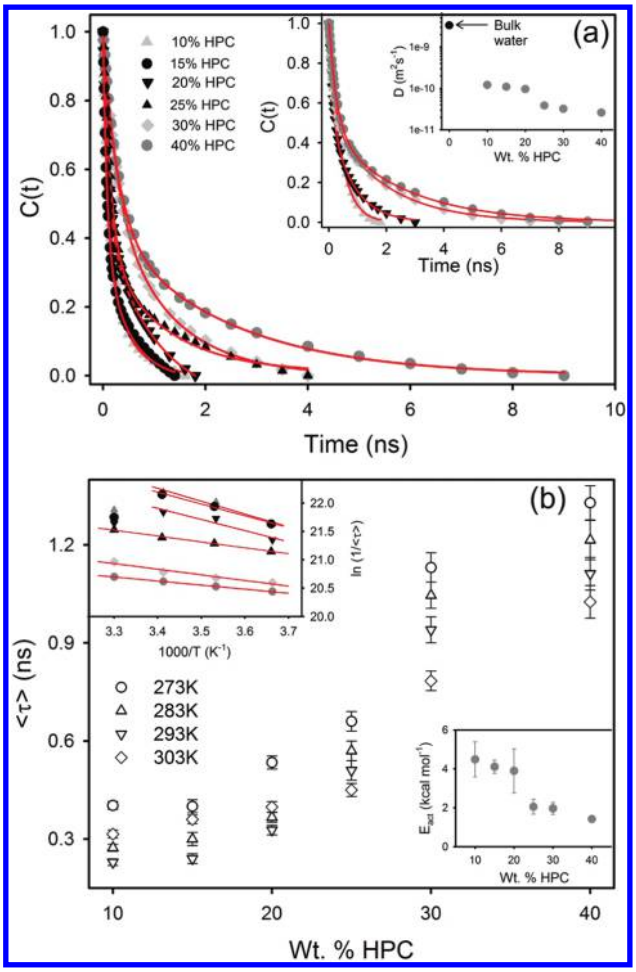

Figure 3. (a) Solvent correlation function, $C(t)$ of C-500 in water-HPC mixtures (with HPC wt % of 10, 15, 20, 25, 30, and 40%) at 293 K. The solid lines are biexponential fittings of the data points. Representative $C(t)$ plots for 10, 20, 30, and 40% HPC solutions at 273 K are presented in the inset. Diffusion coefficients (D) of water in the HPC-water mixture as a function of HPC concentration at 293 K are shown in the inset. The value for bulk water is shown as a black circle. (b) Average solvent relaxation time constants ($<\tau>$) of C-500 in HPC-water mixtures at different temperatures are shown as a function of HPC concentration. Arrhenius plots for different HPC concentrations are shown in the inset. The symbols represent the same as in part a. The solid lines are the linear fits. The measured activation energy values (E_{act}) at different HPC concentrations are plotted in the lower inset.

probes the coupled rotational-translational motion of water molecules in HPC structural network, which is slower than that probed by the DR study, and the observed retardation clearly points out toward a progressive restriction of the translational motion of water with the onset of cholesteric phase at higher HPC concentrations. In order to get a better outlook toward the hindered motion of water at high HPC concentrations, we measure the time-resolved rotational anisotropy of C-500. Representative illustrations of the anisotropy decays at 293 K for 5, 10, 15, 20, 25, and 30% HPC mixtures are depicted in Figure 4. As can be observed from the figures, the anisotropy decay gets slower as HPC concentration increases. The rotational anisotropy for 5% to 25% HPC could be fitted biexponentially. For 5% HPC, the rotational time constants (τ_r) are 0.12 and 1.3 ns, respectively, with an average time constant $<\tau_r>$ ($=a_1\tau_{r1}+a_2\tau_{r2}$) of 0.46 ns. It is to be noted here that C-500

Table 1. Solvation Time Correlation Parameters for C-500 in the HPC-Water Mixture At Different HPC Concentration and Temperature

temp	a_1	τ_1 (ns)	a_2	τ_2 (ns)	$<\tau>$ (ns)
10% HPC-Water Solution					
273 K	0.11	0.10	0.89	0.44	0.40
283 K	0.71	0.16	0.29	0.55	0.27
293 K	0.65	0.11	0.35	0.45	0.23
303 K	0.43	0.07	0.57	0.5	0.32
15% HPC-Water Solution					
273 K	0.45	0.10	0.55	0.65	0.40
283 K	0.52	0.09	0.48	0.52	0.30
293 K	0.62	0.08	0.38	0.50	0.24
303 K	0.77	0.10	0.23	1.22	0.36
20% HPC-Water Solution					
273 K	0.46	0.14	0.54	0.87	0.53
283 K	0.46	0.08	0.54	0.61	0.37
293 K	0.47	0.08	0.48	0.57	0.33
303 K	0.27	0.07	0.73	0.52	0.40
25% HPC-Water Solution					
273 K	0.65	0.19	0.35	1.52	0.66
283 K	0.67	0.19	0.32	1.36	0.57
293 K	0.65	0.14	0.35	1.2	0.51
303 K	0.68	0.14	0.32	1.1	0.45
30% HPC-Water Solution					
273 K	0.51	0.20	0.49	2.10	1.13
283 K	0.48	0.23	0.52	1.80	1.05
293 K	0.50	0.18	0.50	1.70	0.94
303 K	0.56	0.30	0.44	1.40	0.78
40% HPC-Water Solution					
273 K	0.54	0.28	0.46	2.56	1.33
283 K	0.50	0.24	0.50	2.19	1.22
293 K	0.54	0.27	0.46	2.10	1.11
303 K	0.57	0.23	0.43	2.08	1.03

in water exhibits a very fast rotational anisotropy with a time constant of ~50 ps at this temperature.[36] For the present biexponential decay pattern, the faster time constant is comparable to that of C-500 in bulk water, while the other one defines the relatively slower rotational time constant arising out of the restricted motion of water imposed by the HPC molecular network. At 10% HPC, the decay transient gets slower with time constants of 0.13 and 1.4 ns ($<\tau_r>$ = 0.65 ns). For 15, 20, and 25% HPC solutions the time constants are 0.29 and 3.2 ns; 0.85 and 5.2 ns; and 0.9 and 7.4 ns, respectively. We plot the $<\tau_r>$ values against HPC concentration (Figure 4b), and it is observed that in the HPC concentration range of 15–20% $<\tau_r>$ increases sharply correlating the solvent relaxation dynamics study (Figure 3, Table 1). The $<\tau_r>$ values obtained in this study are in the same order of magnitude as reported for the same probe in the PEG-water mixture[32] and RM with low water content.[30] The estimated rotational time constants (τ_r) allow us to calculate the microviscosity (η) experienced by the probe using the Debye–Stokes–Einstein equation

$$\tau_r = \frac{\eta V}{k_B T} \tag{4}$$

where k_B is the Boltzmann constant, and V is the volume of the fluorophore. Considering the radius of the C-500 molecule to be 3.6 Å[41] and taking τ_r to be the slow component arising out of the rotation of the probe in 'bound water', we estimate a microviscosity value of ~3 cP for 10% HPC solution. This

dx.doi.org/10.1021/jp300428h | J. Phys. Chem. B 2012, 116, 1508–1516

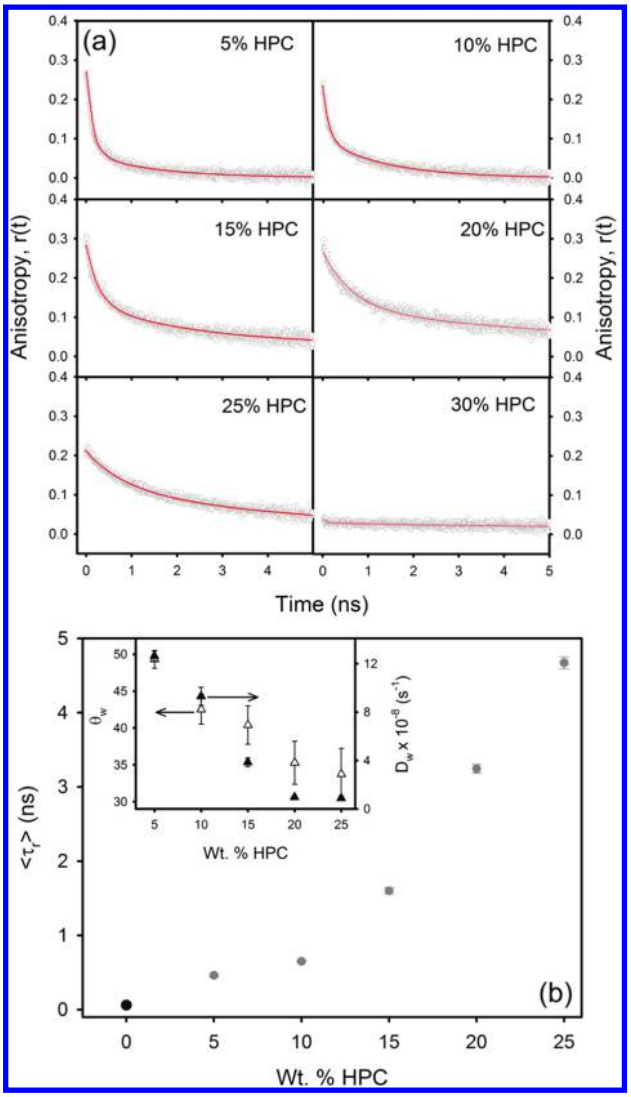

Figure 4. (a) Time resolved rotational anisotropy decays of C-500 in different HPC-water mixtures at 293 K. The solid lines indicate biexponential fittings. (b) Average rotational time constant $<\tau_r>$ as a function of HPC concentration at 293 K. The Wobbling-cone angle (θ_w, hollow symbols) and diffusion coefficient (D_w, filled symbols) as a function of HPC concentration at 293 K are shown in the inset.

value is significantly larger than that of bulk water, and higher than the microviscosity experienced by the same probe in salt solution,[36] however comparable to that obtained in RM systems[30] and in PEG-water system[32] at 293 K. For higher HPC concentrations the microscopic viscosity increases further. This strongly suggests an HPC-water microenvironment, which is much modified compared to that of bulk water as experienced by the probe. For 30 and 40% HPC solutions, the anisotropy decay gets even slower, and the transients could only be fitted considering the presence of an offset, which indicates that the rotation could not be completed within the experimental time window. The observed flat rotational decay transient of the probe in high concentration HPC solution could be explained by considering the rotational motion of the probe in the solution. The rotational anisotropy probes the rotation of the probe (followed by an ultrafast photoexcitation) in the solvent environment. Several modes of rotations are involved and could be realized in the wobbling-in-cone analysis, which concludes that the slow rotational time constant of a probe includes the lateral diffusion of the probe (τ_L) and the overall tumbling motion of the local environment (τ_M), which in turn in connected to the hydrodynamic volume and viscosity of the local environment. In the concentrated HPC solution, both these parameters are high to make τ_{slow} high and thus not measurable within the experimental time window. This makes the offset in the high HPC concentration region. As has been reported earlier, at low hydration level, the polymer chain behaves as a geometrical constraint for rotational motion of water molecules, and their movement is strongly hindered by the polymer chain.[10] This explains the observed slow rotational dynamics and clearly identifies the onset of the appearance of a crystalline phase in which the rotation of the probe essentially freezes, as has also been observed in AOT aqueous lamellar systems using the same probe molecule.[34] We analyze the biexponential anisotropy decay using a wobbling-in-cone model[30,42,43] (Figure 4b, inset) and found that the semicone angle of the wobbling motion decreases from 49.3° for 5% HPC to 33.7° for 25% HPC whereas the diffusion coefficient for the wobbling motion decreases by an order of magnitude (12.6×10^{-8} s^{-1} to 8.8×10^{-9} s^{-1}) on increasing the HPC concentration from 5% to 25% at 293 K. The observed decrease in the semicone angle and diffusion coefficient strongly confirms the restriction imposed on the wobbling motion of water molecules with increasing HPC concentration.

The slow solvation relaxation time constant (τ_2) corresponds to the diffusional motion of the probe in the water-HPC network, and this allows us to estimate the diffusion coefficient (D) of the aqueous environment at the interface. The magnitude of D is directly related to the rms distance $<z^2>^{1/2}$ traveled by the probe in time t by the relation, $<z^2> = 2Dt$. The rms distance can be approximated to as thickness of the bound water layer, and for hydrophobic polymers, this has been reported to be equal to 3.3 Å.[44] Assuming that only the slower solvation time constant (τ_2) is associated with the diffusional motion of the probe, we calculate D and plot it against HPC concentration (Figure 3a, inset). The diffusion coefficient is estimated to be 12.1×10^{-11} m^2 s^{-1} for 10% HPC, while it reduces to 2.6×10^{-11} m^2 s^{-1} for 40% HPC mixture. The observed D values are in good agreement with those reported for other polymer−water systems and are also reported to decrease with increasing polymer concentration.[44,45] A previous MD simulation study[44] shows that translational diffusion coefficient for water molecules near the ether oxygen group of PEG is $\sim 2 \times 10^{-11}$ m^2 s^{-1}, which corresponds well to the obtained D values in the present study at high HPC concentrations, while that in the bulk is $\sim 3.3 \times 10^{-9}$ m^2 s^{-1}. The present results thus reflect formation of enhanced structure beyond 20% HPC in which the translational freedom of water near the polymer surface gets significantly reduced, which is well illustrated by a low value of D. As evidenced from the figure, the decrease in D suffers a transition beyond 20% HPC concentration, a result that corresponds to those obtained from solvation dynamics and rotational anisotropy measurements and signifies the onset of a microscopic phase transition. It could be mentioned here that the slow relaxation process is principally associated with the coupled rotational-translational motion of the solvent molecules, a retardation of both the motions with increasing HPC concentrations is manifested with the phase change.

We now investigate the energetic of the relaxation process involved and in order to estimate the same we perform the time-resolved study at four different temperatures namely 273,

dx.doi.org/10.1021/jp300428h | J. Phys. Chem. B 2012, 116, 1508−1516

283, 293, and 303 K. Measurements at higher temperatures have not been carried out in order to avoid macroscopic phase separation. All the obtained $C(t)$ curves are fitted biexponentially, and the results are summarized in Table 1 and Figure 3b. A few representative $C(t)$ curves for 10, 20, 30, and 40% HPC at 273 K are also shown in the inset of Figure 3a. As observed from Figure 3b and Table 1, the average solvation time constant, $<\tau>$ decreases gradually with increasing temperature with three exceptions at 313 K with 10, 15, and 20% HPC. This observed phenomenon of temperature induced decrease in the relaxation time constant is consistent with an earlier report of HPC-water[21] and PEG-water mixtures[32] and AOT lamellar systems.[34] While the study on HPC[21] is more centered on the dynamics of free water, the PEG-water,[30] AOT lamellar,[34] and the present studies are essentially involved with the slow solvation dynamics, and both processes show the same trend. The accelerated solvation dynamics could be attributed to the temperature induced conversion of 'bound' to 'free' or 'bulk' type water molecules present in the system.[46,47] Such temperature dependency is also observed in rotational anisotropy studies wherein anisotropy decays get faster when temperature is increased (figures not shown). For example, in 10% HPC the fitted rotational time constants are 0.23 and 3.2 ns at 273 K, whereas at 303 K these change to 0.09 and 1.0 ns, respectively. A similar decrease is also noted in case of other solutions.

As corresponds to the other restricted systems studied earlier,[30,32,34] we assume the present system to obey an Arrhenius type of model for the solvation process and fit the time-resolved $C(t)$ data in the following equation

$$\frac{1}{<\tau>} \approx k = Ae^{-E_{act}/RT} \tag{5}$$

where E_{act} is the Arrhenius activation energy for the process, and A is a pre-exponential factor. We plot $\ln(1/<\tau>)$ against $1/T$ for all the four systems (Figure 3b, inset). Good linear fits are obtained for 30 and 40% HPC systems, while for 10, 15, and 20% HPC a deviation from linearity is observed at 303 K. The reason for this deviation is not properly understandable; however, increased hydrophobicity of the systems at higher temperature might well be responsible for the observed deviation. From the slopes of the curves, we calculate the E_{act} values of 4.5 ± 0.9, 4.1 ± 0.3, 3.9 ± 1.1, 2.05 ± 0.4, 2.0 ± 0.3, and 1.4 ± 0.1 kcal mol^{-1} for 10, 15, 20, 25, 30, and 40% HPC systems, respectively. The E_{act} values obtained for 10, 15, and 20% systems are in excellent agreement with those obtained for identical systems using DR studies.[21] These values are also in good agreement with those obtained for microheterogeneous systems like RM,[30] water-PEG mixture,[32] AOT aqueous lamellar system,[34] etc. using the same probe molecule. The free energy change associated with the relaxation process (ΔG^*) could be estimated using an Eyring model

$$\frac{1}{<\tau>} \approx k = \frac{h}{k_B T} e^{-\Delta G^{\#}/RT} \tag{6}$$

and we obtain $\Delta G^{\#}$ values of 3.9, 3.5, 3.2, 1.5, 1.4, and 0.8 kcal mol^{-1}, respectively. An interesting feature is observed when E_{act} is plotted against HPC concentration (Figure 3b, inset) that E_{act} changes only marginally at low HPC concentration region (10 to 20% HPC), which is in good agreement to what has been obtained by Sudo et al.[21] using DR technique, and at high HPC (≥25%) concentration it decreases considerably, a phenomenon strikingly opposite to what has been obtained in the DR studies.[21] This apparently opposing phenomenon is enrooted in the two different relaxation processes probed by Sudo et al. and us. While the former one probes the fast relaxation process of the "free" water molecules our study is mainly aimed toward the slow moving "bound" type water molecules only, and quite intuitively the present decrease in E_{act} resembles an identical observation in AOT RM systems when the water content is decreased.[30] In order to investigate the reason behind the decrease in E_{act} with increasing HPC content, let us first discuss the structure of water in HPC as the concentration of HPC changes. The main chain of the HPC molecule behaves as a semirigid segment in aqueous solution, and the side chains behave in a more flexible way.[21,48] The side chain has an O−H group which can form a hydrogen bond with neighboring HPC as well as water molecules. HPC with its high degree of hydroxypropyl substitution has only a few available hydrophilic sites to create a strong interaction with water molecules. At low concentration HPC acts as a hydrophilic polymer forming an isotropic solution, and as the concentration increases it exhibits a hydrophobic behavior forming a cholesteric LC network structure, which also changes its interaction with water accordingly. The hydrogen bonding between HPC and water prevails at low concentration wherein water can form small clusters, and the solvation process is slower compared to bulk water due to the heteromolecular hydrogen bonded water structure. These water molecules essentially act as "bound water" and contribute to the slow relaxation process (Table 1). The activation energy values obtained is thus very similar to that obtained in the case of other restricted environments like micelles, RM, vesicles, lamellar systems, etc. and smaller than that of pure water. With increasing concentration HPC molecules start forming an intermolecular hydrogen bonded cholesteric structure causing the viscosity of the system to increase significantly, and the polymer solution turns hydrophobic in nature. This ruptures a fraction of HPC-water hydrogen bonds and results in a number of water molecules restricted in the structured HPC network. This preferentially reduces the fraction of bulk water molecules present in the solution and slows down the solvation dynamics. On the other hand, it also sets some water molecules 'free', and the relaxation time probed by Sudo et al.[21] in the high frequency region is exhibited by these 'free water' molecules and due to the less abundance of heteromolecular water-HPC type hydrogen bonding in this phase, the E_{act} reaches a value similar to that of pure water and saturates at HPC concentration above 40%. In our present study, owing to the specific excitation of C-500 we preferentially probe the transition of water molecules at the HPC-water interface. At low HPC (≤20%) content it views the bound to bulk water transition which has an activation energy of 4−5 kcal mol^{-1} and corresponds significantly with the obtained values. On the other hand, at high HPC concentrations (≥25%), it envisages the "interfacially bound" to "interfacially free" water transition, which typically has an energy difference of 1.3−2 kcal mol^{-1}.[46] The observed E_{act} values at high HPC concentrations are thus in excellent agreement with this transition. It could also be noted here that with increasing temperature the aqueous solution of HPC turns hydrophobic. This in turn increases the possibility of the formation of intermolecular hydrogen bond network between HPC molecules, and this perhaps slows down the solvation time constants for 10, 15, and 20% HPC solutions at 303 K (Table 1).

dx.doi.org/10.1021/jp300428h | J. Phys. Chem. B 2012, 116, 1508−1516

In order to understand whether the "bound" to "bulk" type water transition shares the major contribution in the accelerated solvation dynamics at elevated temperatures, we measure the excitation spectra of HPC-water mixtures at different temperatures. As per our discussion earlier, the deconvoluted spectra provide information on the relative amount of water of the two different 'species' existing in the system. The temperature induced population ratio thus could lead us to an estimation of the energy barrier between the two 'species' of water. Let us first consider an equilibrium between 'bound' and 'bulk' type of water molecules present in the system

$$\text{water}_{\text{bound}} \rightleftarrows \text{water}_{\text{bulk}} \tag{7}$$

and the corresponding population be denoted as n_{bound} and n_{bulk}. We now consider a simple Boltzmann type of distribution for both types of water species

$$n_{\text{bound}} = n_0 e^{-E_{\text{bound}}/RT} \tag{8}$$

and

$$n_{\text{bulk}} = n_0 e^{-E_{\text{bulk}}/RT}$$

this leads us to the ratio,

$$\frac{n_{\text{bound}}}{n_{\text{bulk}}} = e^{-\Delta E/RT} \tag{9}$$

where ΔE stands for the energy difference between E_{bound} and E_{bulk}, which in principle be approximated to be equivalent to the activation energy E_{act} estimated from the solvation studies. To make an estimate of ΔE, we deconvolute temperature dependent excitation curves of two samples, namely 10% and 40% HPC. A representative depiction of deconvolution for 40% HPC solution at 273 and 303 K are presented in Figure 1c. We approximate that the excitation peak of C-500 in 'bulk-water' does not suffer appreciable change in this temperature range and fix the bulk water peak at 390 nm while deconvoluting all the spectra. We plot $\ln(n_{\text{bound}}/n_{\text{bulk}})$ against $1/T$ for the two systems (Figure 1d), and from the slopes, we calculate the ΔE values to be 4.2 and 1.0 kcal mol^{-1} for 10% and 40% HPC solution, respectively. These values are in striking correspondence with the obtained E_{act} values estimated from solvation studies. This strongly supports our notion that the observed change in E_{act} is principally governed by the interconversion of the two types of water species present in the system.

Finally, we explore the effect of the restriction imposed by the structure of HPC on the activity of water. We measure the reaction kinetics of benzoyl chloride (BzCl) in water-HPC mixtures at different HPC concentrations, and the results are depicted in Figure 5. Solvolysis of BzCl is essentially a solvent mediated reaction in which water acts as a nucleophile, and the rate of the reaction is primarily governed by the stability of the intermediate acylium carbocation, which in turn is dependent on the polarity of the environment.[49] As evidenced from the figure, the rate of reaction slows down with increasing HPC concentration; for 5% HPC the rate is 0.12 s^{-1}, while for 10% it is 0.07 s^{-1}; however, with 20% and higher HPC concentrations, it decreases rapidly to a value of $\sim 6 \times 10^{-3}$ s^{-1}. Note that due to the very high absorption of cellulose in this region, we could not measure the kinetics for 40% HPC solution. It is worth noting here that the rate constant in water is 1.1 s^{-1}, and it gets reduced by 3−5 orders of magnitude in RMs and polymer solutions depending upon the extent of confinement

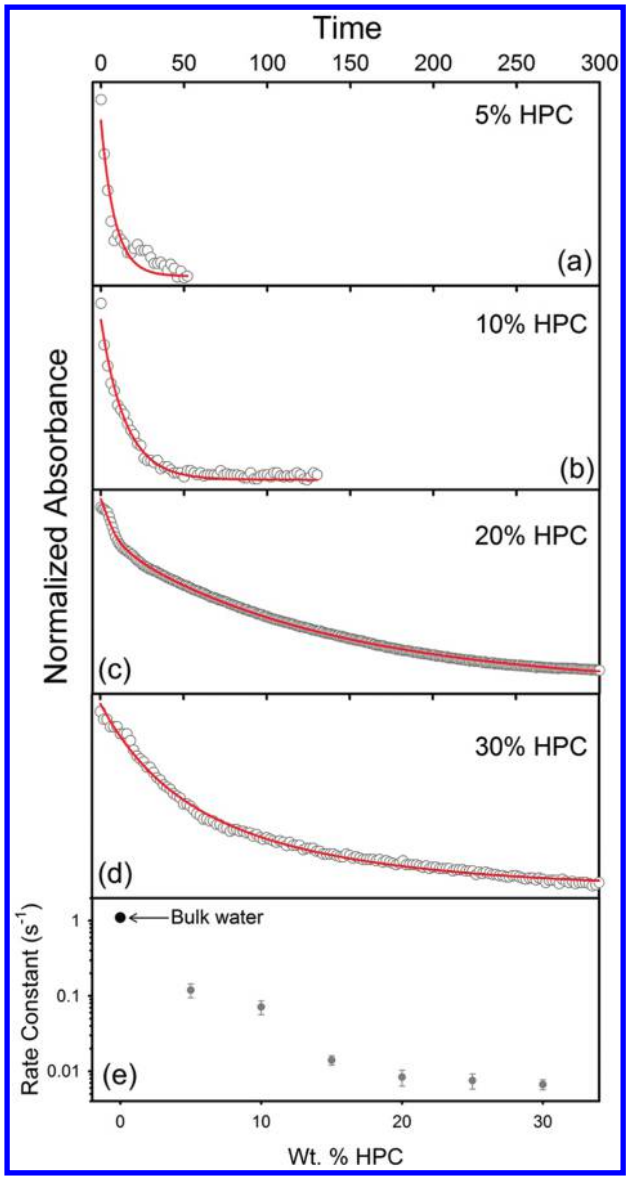

Figure 5. (a-d) Kinetics of BzCl hydrolysis in HPC-water mixtures at different HPC concentrations as measured from the time-resolved decrease in absorbance. The solid lines are the exponential fits of the data. (e) Rate constant of the hydrolysis reaction of benzoyl chloride at different HPC concentrations. The value for bulk water is shown with a black circle.

imposed.[32,33,50] The observed rate is thus slower than that of bulk water, indicating poor nucleophilicity and/or reduced polarity of the environment. Solvation dynamics and anisotropy studies have clearly identified restriction of the translational motion of water owing to hetromolecular hydrogen bonding, which correlates the observed kinetics data. It is interesting to note that the observed reaction rate at low HPC concentrations is an order of magnitude slower than that in water; however, at and beyond 20% HPC it gets another order of magnitude slower. Steady state emission results have clearly indicated a progressive blue shift of the emission maximum of C-500 with HPC concentration (Figure 1a), which in turn indicates a reduced polarity of the microenvironment, a situation unfavorable for the product formation. The further decrease of the reaction rate at 20% HPC concentration could be anticipated with the onset of the hydrophobicity of the polymer

dx.doi.org/10.1021/jp300428h | J. Phys. Chem. B 2012, 116, 1508−1516

as well as the cholesteric structure formation in HPC coupled with the imposed restriction on water molecules within such structures as evidenced from solvation dynamics and anisotropy studies.

CONCLUSION

The present time-resolved spectroscopic study reveals that the dynamics of water relaxation undergoes a characteristic transition beyond 20% HPC concentration, wherein a microscopic phase transition between isotropic to cholesteric phase sets in. This phenomenon is also supported by steady state emission and excitation studies, and a deconvolution of the excitation spectra clearly indicates transition between two 'species' of water. The calculated activation energy for water relaxation (E_{act}) resembles those of other confined systems at low HPC concentrations; however, at higher HPC concentrations, it decreases significantly. This could be explained by the change in the nature of hydrogen bond structure in the water-HPC mixture at higher HPC concentration. The restriction imposed by the structure of HPC on the rotation of the fluoroprobe is also evident from time-resolved rotational anisotropy measurements. Finally the alteration in structure and dynamics of water molecules in the mixture is observed to affect the reactivity of water in the mixture.

AUTHOR INFORMATION

Corresponding Author

*Phone: 91-33-23355706. Fax: 91-33-23353477. E-mail: rajib@bose.res.in.

Notes

The authors declare no competing financial interest.

ACKNOWLEDGMENTS

P.K.V. thanks CSIR for a research fellowship.

REFERENCES

(1) Ball, P. *Chem. Rev.* **2008**, *108*, 74.
(2) Pal, S. K.; Zewail, A. H. *Chem. Rev.* **2004**, *104*, 2099.
(3) Alvarez-Lorenzo, C.; Gómez-Amoza, J. L.; Martínez-Pacheco, R.; Souto, C.; Concheiro, A. *Eur. J. Pharm. Biopharm.* **2000**, *50*, 307.
(4) Chang, Y. P.; Karim, A. A.; Seow, C. C. *Food Hydrocolloids* **2006**, *20*, 1.
(5) Yakimets, I.; Wellner, N.; Smith, A. C.; Wilson, R. H.; Farhat, I.; Mitchell, J. *Polymer* **2005**, *46*, 12577.
(6) Giraudier, S.; Hellio, D.; Djabourov, M.; Larreta-Garde, V. *Biomacromolecules* **2004**, *5*, 1662.
(7) Petersson, M.; Lorén, N.; Stading, M. *Biomacromolecules* **2005**, *6*, 932.
(8) Shinouda, H. G.; Moteleb, M. M. A. *J. Appl. Polym. Sci.* **2005**, *98*, 571.
(9) Einfeldt, J.; Meißner, D.; Kwasniewski, A. *Cellulose* **2004**, *11*, 137.
(10) Ryabov, Y. E.; Feldman, Y.; Shinyashiki, N.; Yagihara, S. *J. Chem. Phys.* **2002**, *116*, 8610.
(11) Yakimets, I.; Paes, S. S.; Wellner, N.; Smith, A. C.; Wilson, R. H.; Mitchell, J. R. *Biomacromolecules* **2007**, *8*, 1710.
(12) *Hydroxypropylcellulose: chemical and physical properties*; Hercules Inc.: Wilmington, DE, 1971.
(13) Werbowyj, R. S.; Gray, D. G. *Macromolecules* **1980**, *13*, 69.
(14) Aspler, J. S.; Gray, D. G. *Macromolecules* **1981**, *14*, 1546.
(15) Yamazaki, I.; Winnik, F. M.; Winnik, M. A.; Tazuke, S. *J. Phys. Chem.* **1987**, *91*, 4213.
(16) Fortin, S.; Charlet, G. *Macromolecules* **1989**, *22*, 2286.
(17) Streletzky, K. A.; Phillies, G. D. J. *J. Polym. Sci., Part B: Polym. Phys.* **1998**, *36*, 3087.
(18) Mustafa, M. B.; Tipton, D. L.; Barkley, M. D.; Russo, P. S.; Blum, F. D. *Macromolecules* **1993**, *26*, 370.
(19) Phillies, G. D. J.; Quinlan, C. A. *Macromolecules* **1995**, *28*, 160.
(20) Phillies, G. D. J.; O'Connell, R.; Whitford, P.; Streletzky, K. A. *J. Chem. Phys.* **2003**, *119*, 9903.
(21) Sudo, S. *J. Phys. Chem. B* **2011**, *115*, 2.
(22) Immaneni, A.; Kuba, A. L.; McHugh, A. J. *Macromolecules* **1997**, *30*, 4613.
(23) Beheshti, N.; Bu, H.; Zhu, K.; Kjøniksen, A.-L.; Knudsen, K. D.; Pamies, R.; Cifre, J. G. H.; García de la Torre, J.; Nyström, B. *J. Phys. Chem. B* **2006**, *110*, 6601.
(24) Bu, Z.; Russo, P. S. *Macromolecules* **1994**, *27*, 1187.
(25) Wojciechowski, P.; Joachimiak, A.; Halamus, T. *Polym. Adv. Technol.* **2006**, *14*, 826.
(26) Wirick, M. G.; Waldman, M. H. *J. Appl. Polym. Sci.* **1970**, *14*, 579.
(27) Samuels, R. J. *J. Polym. Sci., Part B: Polym. Phys.* **1969**, *7*, 1197.
(28) Sugimoto, H.; Miki, T.; Kanayama, K.; Norimoto, M. *J. Non-Cryst. Solids* **2008**, *354*, 3220.
(29) Mitra, R. K.; Sinha, S. S.; Pal, S. K. *J. Phys. Chem. B* **2007**, *111*, 7577.
(30) Mitra, R. K.; Sinha, S. S.; Pal, S. K. *Langmuir* **2008**, *24*, 49.
(31) Mitra, R. K.; Sinha, S. S.; Verma, P. K.; Pal, S. K. *J. Phys. Chem. B* **2008**, *112*, 12946.
(32) Verma, P. K.; Mitra, R. K.; Pal, S. K. *Langmuir* **2009**, *25*, 11336.
(33) Verma, P. K.; Makhal, A.; Mitra, R. K.; Pal, S. K. *Phys. Chem. Chem. Phys.* **2009**, *11*, 8467.
(34) Verma, P. K.; Saha, R.; Mitra, R. K.; Pal, S. K. *Soft Matter* **2010**, *6*, 5971.
(35) O'Connor, D. V.; Philips, D. *Time correlated single photon counting*; Academic Press: London, 1984.
(36) Banerjee, D.; Verma, P. K.; Pal, S. K. *Photochem. Photobiol. Sci.* **2009**, *8*, 1441.
(37) Majumder, P.; Sarkar, R.; Shaw, A. K.; Chakraborty, A.; Pal, S. K. *J. Colloid Interface Sci.* **2005**, *290*, 462.
(38) Koti, A. S. R.; Krishna, M. M. G.; Periasamy, N. *J. Phys. Chem. A* **2001**, *105*, 1767.
(39) Fee, R. S.; Maroncelli, M. *Chem. Phys.* **1994**, *183*, 235.
(40) Sudo, S.; Oshiki, N.; Shinyashiki, N.; Yagihara, S. *J. Phys. Chem. A* **2007**, *111*, 2993.
(41) Nad, S.; Pal, H. *J. Phys. Chem. A* **2003**, *107*, 501.
(42) Lipari, G.; Szabo, A. *J. Am. Chem. Soc.* **1982**, *104*, 4546.
(43) Lipari, G.; Szabo, A. *Biophys. J.* **1980**, *30*, 489.
(44) Tasaki, K. *J. Am. Chem. Soc.* **1996**, *118*, 8459.
(45) Faraone, A.; Magazù, S.; Maisano, G.; Migliardo, P.; Tettamanti, E.; Villari, V. *J. Chem. Phys.* **1999**, *110*, 1801.
(46) Pal, S.; Balasubramaian, S.; Bagchi, B. *J. Phys. Chem. B* **2003**, *107*, 5194.
(47) Balasubramaian, S.; Pal, S.; Bagchi, B. *Phys. Rev. Lett.* **2002**, *89*, 115505.
(48) Evmenenko, G.; Yu, C.-J.; Kewalramani, S.; Dutta, P. *Langmuir* **2004**, *20*, 1698.
(49) Bentley, T. W.; Carter, G. E.; Harris, H. C. *J. Chem. Soc., Chem. Commun.* **1984**, 387.
(50) Garcia-Rio, L.; Leis, J. R.; Iglesias, E. *J. Phys. Chem.* **1995**, *99*, 12318.